J. Fluid Mech. (1990), *vol.* 213, *pp.* 111–126
Printed in Great Britain

High-Rayleigh-number convection in a horizontal enclosure

By R. J. GOLDSTEIN[1], H. D. CHIANG[2] AND D. L. SEE[3]

[1] Department of Mechanical Engineering, University of Minnesota, Minneapolis, MN 55455, USA

[2] Textron Lycoming, Stratford, CT 06497, USA

[3] Canterra Energy Ltd, Calgary, Alberta T2P 2K7, Canada

(Received 12 September 1988 and in revised form 1 August 1989)

A review of the literature on natural convection in a horizontal layer heated from below shows the need for reliable data at high Rayleigh number (Ra) to determine the asymptotic Nusselt number (Nu) variation with Rayleigh number. The present study expands the data base by the use of an electrochemical mass transfer technique to determine the asymptotic dependence of the Sherwood number (Sh) on Ra at high Schmidt number (Sc). The results of the present study give $Sh = 0.0659\,Ra^{\frac{1}{3}}$ for $Sc \approx 2750$, $3 \times 10^9 < Ra < 5 \times 10^{12}$. Using the heat-mass transfer analogy, this indicates the high Prandtl number variation of Nu with Ra.

1. Introduction

Natural convection arises from the presence of density gradients within a fluid in a body force (generally a gravitational) field. This buoyancy driven convection occurs in many natural and human made environments. Density gradients due to a non-uniform temperature or species distribution are the driving forces of the fluid motion, and the density and velocity fields are coupled by complex relationships. Such flows can cause the transport of heat and/or mass.

Natural convection within a horizontal layer with an unstable density gradient is of both engineering and scientific significance. Many books and reviews consider such flows. Numerous theoretical and experimental studies have been performed, with some primarily directed towards the stability and hydrodynamics, while others are more concerned with the heat and/or mass transfer process. A list of relevant review articles and papers is given at the end of the References.

For a horizontal layer of infinite horizontal extent with isothermal (or uniform concentration) boundaries and a top-heavy density gradient ('heated from below'), the primary parameter influencing the flow field is the Rayleigh number (Ra). Such flows are often called Rayleigh–Bénard convection. A critical Rayleigh number is known, through both theoretical analysis and experimental observaton, below which the transport of heat is by conduction (or the transport of mass by diffusion) and the fluid is essentially motionless. This critical Rayleigh number for the onset of convection has a value of about 1708 and is independent of the Prandtl number (Pr) or Schmidt number (Sc). Increasing the Rayleigh number beyond the critical value, the first mode of convective motion is generally a steady two-dimensional flow field in the form of rolls. With a further increase in the Rayleigh number, the fluid motion, in a fluid of moderate or high Pr, will progress from two-dimensional to three-

dimensional steady state flow, then to time-dependent flow and finally become turbulent. These subsequent transitions have a strong Prandtl number dependence (Krishnamurti 1973; Busse 1981).

For Prandtl numbers less than about 5, an increase in Rayleigh number leads to a direct transition from steady two-dimensional rolls to time-dependent flow. The Rayleigh number for this transition from steady to time-dependent flows is an increasing function of the Prandtl number, ranging from below 2500 at $Pr \approx 0.01$ to about 20000 at $Pr \approx 5$ (Krishnamurti 1973). At higher Prandtl number, an increase in Rayleigh number leads to a transition from steady two-dimensional rolls to a steady three-dimensional flow field. This second transition occurs at $Re \approx 2 \times 10^4$, independent of the Prandtl number for $Pr > 5$. The three-dimensional flow field manifests itself in the form of additional roll-like structures perpendicular to the basic rolls (bimodal convection).

As the Rayleigh number is increased further, transition to time-dependent convection occurs. There is a Prandtl-number effect on this transitional Rayleigh number. However, there is no general agreement about the Prandtl-number dependence for the onset of time-dependent flow. For $Pr > 50$, Krishnamurti (1973) observed this third transition at a Rayleigh number of about 6×10^4. At even higher Rayleigh number, the flow becomes chaotic. Krishnamurti's curves indicate the flow to be turbulent at Rayleigh number of about 10^4 for Prandtl number around unity, about 10^5 for water ($Pr \approx 7$), and about 10^6–10^7 for higher Prandtl number fluids.

The relationship between the Nusselt number (Nu), or the Sherwood number (Sh) for mass transfer, and the Rayleigh number is of fundamental importance. At high Rayleigh number, the asymptotic variation of the Nusselt number as a function of the Rayleigh number has been the subject of many theoretical and numerical studies.

For fully-turbulent heat transfer in horizontal layer, the $\frac{1}{3}$-power law in which the heat transport is independent of the layer thickness is often assumed;

$$Nu = KRa^{\frac{1}{3}}, \tag{1}$$

where the characteristic length used in the definition of both Nu and Ra is L, the fluid-layer thickness or height. The $\frac{1}{3}$-power law can be obtained from the application of the mixing-length theory to horizontal layers developed by Priestley (1959). Extension of the mixing-length model by Kraichnan (1962) indicates K to be a function of the Prandtl number ($K = 0.17Pr^{\frac{1}{3}}$) for $Pr < 0.1$ and $K = 0.089$ for $Pr > 0.1$. However, experimental measurements often result in a best fit correlation,

$$Nu = cRa^m, \tag{2}$$

with the exponent, m, slightly less than $\frac{1}{3}$.

Malkus (1954*b*) proposed a model to predict the upper limit to the heat transport in turbulent convection. Assuming that the mean temperature gradient is non-positive and the highest vertical wavenumber of the series expansion of the mean velocity and temperature profiles is marginally stable, he truncated the series and obtained a maximum amount of heat transfer (see also Spiegel 1962; Townsend 1962). Expanding on the idea of Malkus, Howard (1963) proposed a theory, solving a variational problem that satisfies the boundary conditions and the continuity equation. The problem does not satisfy the Boussinesq equation exactly, but is subject to two integral constraints derived from the Boussinesq equation (the 'power integrals'). A complete solution of the variational problem will give an upper bound

for the convective heat flux. Elaborations and expansions (Busse 1969; Chan 1971; Strauss 1976) lead to the turbulence model called the optimum theory of turbulence (Busse 1978*a*). The first upper bound predicted by Howard (1963) is

$$Nu_{\max} = (Ra/248)^{\frac{3}{8}} \tag{3}$$

and an improved upper bound by Chan (1971) gives, for $Pr \to \infty$ and $Ra \to \infty$,

$$Nu_{\max} = 0.152\,Ra^{\frac{1}{3}}. \tag{4}$$

Numerical calculations using finite difference procedures have been attempted by various investigators (Deardorff 1965; Deardorff & Willis 1965; Fromm 1965; Lipps 1976). Their solutions do not go beyond $Ra = 10^7$. However, Fromm arrives at a slope of $\frac{1}{3}$ for free boundaries and a slope of 0.296 for rigid boundaries, suggesting perhaps that with rigid boundaries, fully turbulent behaviour occurs at Rayleigh number greater than 10^7.

A phenomenological model for the mechanism of turbulent convection in horizontal enclosures at high Rayleigh number was proposed by Howard (1966). His model, and the classical investigation by Townsend (1959) together with the observations by Chu & Goldstein (1973) give rise to the now popular concept of thermals. An attempt to verify Howard's model has been made (Sparrow, Husar & Goldstein 1970) but more work is needed.

Another approach starts from the so-called 'mean-field equation' where the nonlinear terms in fluctuating quantities are omitted (see, for example, Malkus 1954*a*; Herring 1964). To improve on the mean field equation, some approximations for the neglected nonlinear terms are added. These models are loosely called 'modal equations' (Roberts 1966; Spiegel 1967; Gough, Spiegel & Toomre 1975).

Herring's calculation (1964) for rigid boundaries yields the $\frac{1}{3}$-power law at large Rayleigh number. His solution for the special case of infinite Prandtl number indicates $K = 0.115$. Roberts (1966) employs an asymptotic expansion technique to introduce the nonlinear interactions. A first-order expansion is used to study the behaviour at moderate Rayleigh number. At large Rayleigh number, a second-order expansion is used by Stewartson in the Appendix of Roberts' paper to give

$$Nu \to 0.2782(Ra^2 \log Ra^2)^{\frac{1}{5}}. \tag{5}$$

No Prandtl-number effect on this asymptote is predicted. Gough *et al.* (1975) employ the Galerkin method, truncating the orthogonal expansion of the velocity and temperature fields. With only one term of the expansion included, the resulting equations reproduce some of the qualitative behaviour of cellular convection. At very high Rayleigh numbers, they find a Prandtl-number dependence in the *Nu–Ra* relation.

Several analytical models have been proposed recently (Long 1976; Canuto & Goldman 1985; Arpaci 1986; Howard & Krishnamurti 1986). Long proposed a model that is based on simplifications in the boundary layers and a buoyancy-defect law in the interior layer. His results give a closed form relationship between *Nu*, *Ra* and *Pr* involving three unknown constants. More recently, Canuto & Goldman (1985) proposed a model for large-scale turbulence using a closure that depends on the growth rate of the instability-generating turbulence. The model predicts the $\frac{1}{3}$-power law with a Prandtl-number dependence for the constant K: $K = 0.044$ for $Pr = 6.8$ and $K = 0.061$ for $Pr = 1000$. Arpaci (1986) extended the concept of Taylor's and

Kolmogorov's microscale to develop a thermal microscale for buoyancy-driven flows. Applying the concept to turbulence in horizontal enclosures, he finds

$$Nu = K'\left(\frac{Pr}{1+Pr}Ra\right)^{\frac{1}{3}}. \tag{6}$$

Howard & Krishnamurti (1986) proposed a model for the study of large-scale flow in turbulent convection by truncation of the two-dimensional Boussinesq equation. The model yields some qualitative features of the observed flow fields. No correlation was given.

A summary of analytically obtained correlations for high-Rayleigh-number convections within a horizontal layer is presented in table 1. A companion summary of the high-Rayleigh-number experimental studies using horizontal enclosures is given in table 2.

Measurements of the heat transfer across horizontal enclosures over a range of Rayleigh and Prandtl numbers have been made by many investigators. Yet there is still a paucity of data for the high-Rayleigh-number asymptotes over a wide range of the Prandtl number.

Experiments in mercury ($Pr = 0.025$) have been performed for $Ra < 3.3 \times 10^7$ (Globe & Dropkin 1959; Rossby 1969). Globe & Dropkin's results show a $\frac{1}{3}$-power law whereas Rossby's results indicates $Nu \propto Ra^{0.26}$. For convection in air and helium ($Pr \approx 0.7$), many experimental studies are available. Only a few of these were carried out to high Rayleigh number (Goldstein & Chu 1969; Threlfall 1975; Fitzjarrald 1976). The highest Rayleigh number is 7×10^9, and the power law ($Nu \propto Ra^m$) fits of the data all shown an exponent of less than $\frac{1}{3}$. A recent experiment by Heslot, Castaing & Libchaber (1987) using low-temperature gaseous helium indicates a power-law relationship with an exponent less than one-third at their highest Ra ($\approx 10^{11}$). Similar results of power-law exponent less than $\frac{1}{3}$ are reported for water and acetone ($Pr \approx 5$) up to $Ra \approx 3 \times 10^9$ (Malkus 1954*a*; Globe & Dropkin 1970, private communication; Chu & Goldstein 1973; Garon & Goldstein 1973; Tanaka & Miyata 1980). The experimental results of Goldstein & Tokuda (1980), using water, extends the Rayleigh number range to 2×10^{11}. They did find a $\frac{1}{3}$-power relationship for natural convection in water in a horizontal enclosure at high Ra. Their correlation is,

$$Nu = 0.0556\, Ra^{\frac{1}{3}} \quad (Pr = 6.5). \tag{7}$$

Several studies used high-Prandtl-number fluids (see table 2). The range of Rayleigh numbers is also limited, up to $Ra \approx 10^8$ for $Pr \approx 10$ and only $Ra < 10^6$ for $Pr > 100$.

The object of the present work is to study high-Prandtl-number, high-Rayleigh-number convection in a horizontal layer. The difficulties of achieving high Rayleigh number for a high-Prandtl-number fluid leads to the use of an analogy. An electrochemical system with a high-Schmidt-number (Sc) fluid is used to simulate a high-Prandtl-number heat transfer.

2. The electrochemical technique

Much of this description of the electrochemical technique is taken from Chiang & Goldstein (1990) and Goldstein, Chiang & Sayer (1987). Electrochemical systems employ a diffusion-controlled electrolytic reaction (or pair of reactions) to study transport phenomena. With an externally applied potential across two electrodes, a

Authors	Models	Pr range	Correlations
Priestley (1959)	Mixing length	—	$Nu = \mathrm{K}\, Ra^{\frac{1}{3}}$
Chang (1957)	Conduction layer model	Moderate to high	$Nu = 0.146\, Ra^{\frac{1}{3}}$
Kraichnan (1962)	Mixing length	$Pr < 0.1$	$Nu = 0.17\,(Pr\, Ra)^{\frac{1}{3}}$
		$Pr > 0.1$	$Nu = 0.089\, Ra^{\frac{1}{3}}$
Howard (1963)	Optimum theory	—	$Nu_{\max} = (3\, Ra/64)^{\frac{1}{2}}$
			$Nu_{\max} = (Ra/248)^{\frac{3}{8}}$
Herring (1964)	Mean field equation	$Pr \to \infty$	$Nu = 0.115\, Ra^{\frac{1}{3}}$
Fromm (1965)	Finite difference	—	$Nu \propto Ra^{0.296}$
Howard (1966)	Phenomenological model of thermal	—	$Nu \propto Ra^{\frac{1}{3}}$
Roberts (1966)	Asymptotic expansion	—	$Nu \leqslant 0.2782\,(Ra^2 \log Ra^2)^{\frac{1}{5}}$
Busse (1969)	Optimum theory	—	$Nu_{\max} = (Ra/1035)^{\frac{1}{2}}$
Chan (1971)	Optimum theory	$Pr \to \infty$	$Nu_{\max} = 0.152\, Ra^{\frac{1}{3}}$
Long (1976)	Buoyancy defect law	$Pr = 0.8$	$Nu = \dfrac{0.0524\, Ra^{\frac{1}{3}}}{\{1 - 1.021\,(Ra\, Nu)^{-\frac{1}{12}}\}^{\frac{4}{3}}}$
		$Pr = 6.8$	$Nu = \dfrac{0.043\,56\, Ra^{\frac{1}{3}}}{\{1 - 1.402\,(Ra\, Nu)^{-\frac{1}{12}}\}^{\frac{4}{3}}}$
Canuto & Goldman (1985)	Large-scale turbulence model	$Pr = 6.8$	$Nu = 0.044\, Ra^{\frac{1}{3}}$
		$Pr = 1000.0$	$Nu = 0.061\, Ra^{\frac{1}{3}}$
Arpaci (1986)	Thermal microscale	—	$Nu = [Pr\, Ra/(1+Pr)]^{\frac{1}{3}}$

TABLE 1. Analytical correlations for horizontal layers at high Rayleigh number

Investigators	Correlations	Range of Ra	Approx. Pr, Fluids
Globe & Dropkin (1959)	$Nu = 0.051\,Ra^{\frac{1}{3}}$	2×10^5–3×10^7	0.022, Mercury
Rossby (1969)	$Nu = 0.147\,Ra^{0.247}$	2×10^4–5×10^5	0.024, Mercury
Mull & Reiher (1930) Jakob (1946)	$Nu = 0.077\,Ra^{\frac{1}{3}}$	10^5–10^7	0.7, Air
Willis & Deardorff (1967)	—	10^3–3×10^6	0.7, Air
Goldstein & Chu (1969)	$Nu = 0.123\,Ra^{0.294}$	6×10^5–1×10^8	0.7, Air
Ahlers (1974)	—	10^3–3×10^5	0.6–1.4, Helium
Hollands *et al.* (1975)	—	10^3–4×10^6	0.7, Air
Threlfall (1975)	$Nu = 0.173\,Ra^{0.280}$	4×10^5–2×10^9	0.8, Helium
Fitzjarrald (1976)	$Nu = 0.13\,Ra^{0.30}$	4×10^4–7×10^9	0.7, Air
Heslot *et al.* (1987)	$Nu = 1+0.096\,Ra^{0.333}$	3×10^5–4×10^7	Helium
	$Nu = 1+0.2\,Ra^{0.282}$	4×10^7–10^{11}	—
Malkus (1954*a*)	$Nu \propto Ra^{0.325}$	10^6–3×10^9	5, Water and acetone
Rossby (1969)	$Nu = 0.131\,Ra^{0.30}$	3×10^4–3×10^6	6.8, Water
Globe & Dropkin (private communication)	$Nu = 0.440\,Ra^{0.230}$	4×10^6–2×10^8	4, Water
Chu & Goldstein (1973)	$Nu = 0.183\,Ra^{0.278}$	2×10^5–1×10^8	6, Water
Garon & Goldstein (1973)	$Nu = 0.130\,Ra^{0.293}$	1×10^7–3×10^9	5.5, Water
Tanaka & Miyata (1980)	$Nu = 0.145\,Ra^{0.290}$	3×10^7–4×10^9	6.8, Water
Goldstein & Tokuda (1980)	$Nu = 0.0556\,Ra^{\frac{1}{3}}$	10^9–2×10^{11}	6.5, Water
Schmidt & Silveston (1959)	$Nu = 0.094\,Ra^{\frac{1}{3}}$	3×10^4–4×10^5	35, Silicone oil, AK3
Dropkin & Somerscales (1965)	$Nu = 0.069\,Pr^{0.074}\,Ra^{\frac{1}{3}}$	2×10^5–7×10^8	0.022 – 8000, Mercury, water and silicone oils
Somerscales & Gazda (1968)	$Nu = 0.196\,Ra^{0.283}$	3×10^7–3×10^8	5.5, Silicone oil (0.65 cs)
		7×10^5–1×10^8	18.0, Silicone oil (2 cs)
Rossby (1969)	$Nu = 0.184\,Ra^{0.281}$	4×10^3–3×10^6	200, Silicone oil (20 cs)
Koschmieder & Pallas (1974)	—	10^3–3×10^5	50–1670, Silicone oils (5–200 cs)
Globe & Dropkin (private communication)	$Nu = 0.0665\,Pr^{0.083}\,Ra^{0.335}$	3×10^7–7×10^8	15, Silicone oil (1.5 cs)
		1×10^6–2×10^7	300, Silicone oil (50 cs)
		1×10^5–6×10^5	8000, Silicone oil (1000 cs)
Present study	$Sh = 0.0659\,Ra^{\frac{1}{3}}$	3×10^9–5×10^{12}	$Sc \approx 2750$, Electrochemical mass transfer

TABLE 2. Heat transfer experiments and correlations for horizontal enclosures at high Rayleigh numbers

current will flow through an electrolytic solution from the anode to the cathode. The study of the mass transfer process at the cathode surface can be used to understand electrolytic physical phenomena in their own right or it can be used to predict the corresponding heat transfer process through the appropriate analogy.

The advantages of an electrochemical system over a conventional heat transfer system are: (i) high precision and local measurements are easier to achieve, (ii) large Rayleigh number can be achieved in moderate-sized apparatus, (iii) there is better control of boundary conditions and (iv) sidewall conduction and radiation effects are eliminated. The electrochemical systems normally used all have high Schmidt number (analogous to the Prandtl number), hence, the analogy is limited to high-Prandtl-number fluids.

A wealth of information on electrochemical systems is available. Books by Levich (1962) and Newman (1973) provide extensive coverage. On the application side, reviews by Mizushina (1971) and Wragg (1977) give in-depth surveys of the literature. A review paper by Selman & Tobias (1978) and a recent paper by Chiang & Goldstein (1990) cover the various operating conditions of the technique and their constraints. Interested readers should refer to these papers for more information.

A typical electrochemical system consists of an electrolytic solution as the working fluid, and two electrodes, an anode and a cathode (or cathodes), in the solution at the location(s) of interest. Mass transfer is induced in the solution by applying an external electric potential difference across the electrodes. Positive ions (cations) of the electrolyte move toward the cathode while the negative ions (anions) move toward the anode. The movement of the ions is driven by: (i) diffusion because of the ion-density gradient, (ii) convection if the fluid is in motion, and (iii) migration due to the electric field.

In a heat transfer process, diffusion and convection processes are present, but there is no equivalent to migration. In order to use ionic transport as an analog to the heat transfer process, the ionic migration must be suppressed. This is achieved by the introduction of a second electrolyte – normally called the supporting electrolyte. It is usually in the form of an acid or base with a concentration many times that of the active electrolyte, and selected so that its ions do not react at the electrodes over the range of potential difference used in the experiment. The excess of supporting electrolyte will reduce the migration effect on the charge carrier to the extent that the effect can be accounted for with a small correction or can even be neglected.

With an electrochemical mass transfer system the Rayleigh number is defined by

$$Ra = \frac{g\,\Delta\rho\,L^3}{\rho\nu D_i}, \tag{8}$$

where g is acceleration due to gravity, ρ is fluid density, ν is the kinematic viscosity, D_i is the diffusion coefficient for species i which is the species being transported. For transport across a horizontal layer the characteristic length, L, would be the spacing between the active horizontal surfaces (i.e. the height or thickness of the fluid layer) and $\Delta\rho$ the density difference of the fluid between the anode and cathode.

In the present study, a cupric sulphate–sulphuric acid solution ($CuSO_4$–H_2SO_4–H_2O) is used. With an externally applied electric potential across the electrodes, copper is dissolved from the anode and deposited onto the cathode (metal deposition reaction). Advantages of the copper deposition system (compared to other electrolytic solution for the study of natural convection) are ease of handling, higher densification constant (ratio of density difference for a given concentration difference $-\Delta\rho/\Delta C$) and the greater availability of physical property correlations.

The mass transfer coefficient for species i is

$$h_i = \frac{(N_i'')_{DC}}{\Delta C_i}, \tag{9}$$

where $(N_i'')_{DC}$ is the flux of species i due to diffusion and convection and ΔC_i is the concentration difference of species i across the region of interest.

The dimensionless mass transfer coefficient, the Sherwood number (Sh), is defined by

$$Sh = \frac{h_i L}{D_i}. \tag{10}$$

The total flux at the cathode surface can be determined from Faraday's law,

$$N_i'' = \frac{I}{n_i F}, \tag{11}$$

where I is the current density at the cathode surface, n_i is the valence of the transferred ion, and F is the Faraday's constant.

In the presence of the supporting electrolyte, the migration effect on the active electrolyte is small and approaches zero as

$$\frac{C_{CuSO_4}}{C_{H_2SO_4}} \to 0. \tag{12}$$

Under the constraint that the solution is a dilute solution, the small migration flux, $(N_i'')_{mi}$, can be related to the current density using the transference number, t_i, which is a function of the solution concentration. Then,

$$(N_i'')_{mi} = \frac{t_i I}{n_i F}. \tag{13}$$

Combining (13) with (11) and (12),

$$h_i = \frac{I(1-t_i)}{n_i F \Delta C_i}. \tag{14}$$

In most studies the relevant concentration difference is the difference between the bulk and surface concentrations. The bulk concentration is a constant and can be measured by chemical analysis, but the surface concentration is an unknown. In heat transfer studies, the surface temperature can often be determined from the solid side and assumed to be the same as that of the liquid at the interface. In contrast, direct measurement of surface concentration is generally not feasible. This is resolved by using the 'limiting current' condition. As the externally applied potential across the electrodes is increased, the current increases monotonically until a plateau – on the graph of current *vs.* potential – occurs. At the limiting current, I_{lim}, the concentration of the reacting ions at the cathode surface will be negligible. Hence, measurement of the limiting current density and knowledge that the cathode surface concentration of the reacting ions is almost zero will enable the determination of the mass transfer coefficient by the use of (14). From this, one can infer that the measurement of localized limiting current densities under constant surface potential will yield information on the local mass transfer coefficients. The constant surface potential condition – really constant (zero) wall concentration of the reacting ions – is an analog to the constant temperature boundary condition.

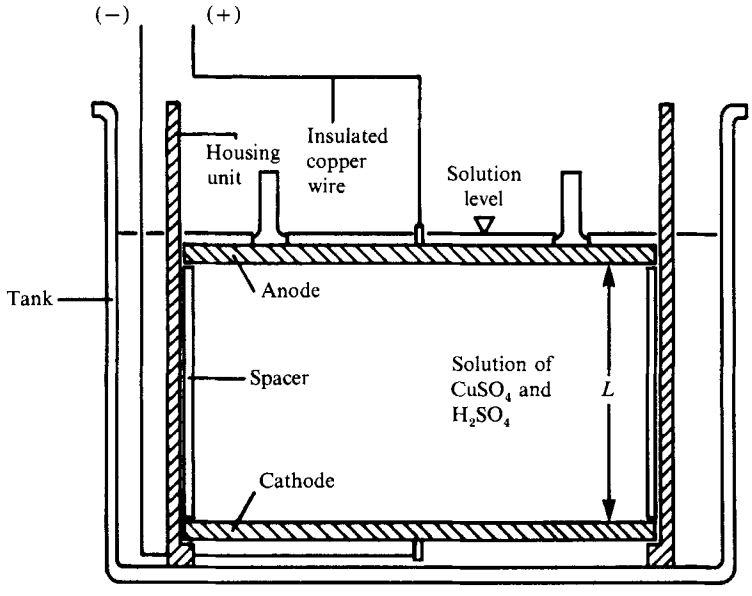

FIGURE 1. Test apparatus.

When applying the electrochemical technique to the study of natural convection within parallel enclosures, the symmetry (or anti-symmetry), with respect to the central plane of the enclosure, is used to infer the concentration at the anode surface. Assuming that the concentration profile at the anode is similar to (really, the reverse of) that at the cathode, the concentration of the cupric ions at the anode surface is twice that of the bulk concentration at the limiting current condition.

To determine the dimensionless parameters of interest, the Sherwood number (analogous to the Nusselt number) and the Rayleigh number, the appropriate physical properties of the working electrolyte are needed. The physical property correlations for the buoyancy-driven copper deposition system have been reviewed and summarized in Chiang & Goldstein (1989).

Since all experimental runs start with the fluid at rest, sufficient time should be allowed for the transient to subside. For horizontal enclosures, the transient time is experimentally determined to be about 10–20 min. The theoretical vertical diffusion time for a horizontal turbulent boundary layer is about 30 min. At a cupric sulphate concentration of about 0.02 M, a run time greater than 10 h is not recommended. A typical experimental run for the present study lasts about 1–2 h. With the copper deposition system used, the fraction of mass transfer by migration is of the order of 1% (included in the analysis) for the range of cupric sulphate concentrations used in this study.

3. Apparatus and procedure

Figure 1 shows a schematic of the apparatus used in the present study. The test chamber includes two copper plate electrodes which are held parallel to each other by a hollow rectangular Plexiglas spacer. The plate–spacer assembly is placed inside a Plexiglas housing unit, and the housing unit immersed in a polyethylene tank containing a solution of cupric sulphate and sulphuric acid. The sidewalls of the test chamber are impermeable, simulating adiabatic walls in the heat transfer case.

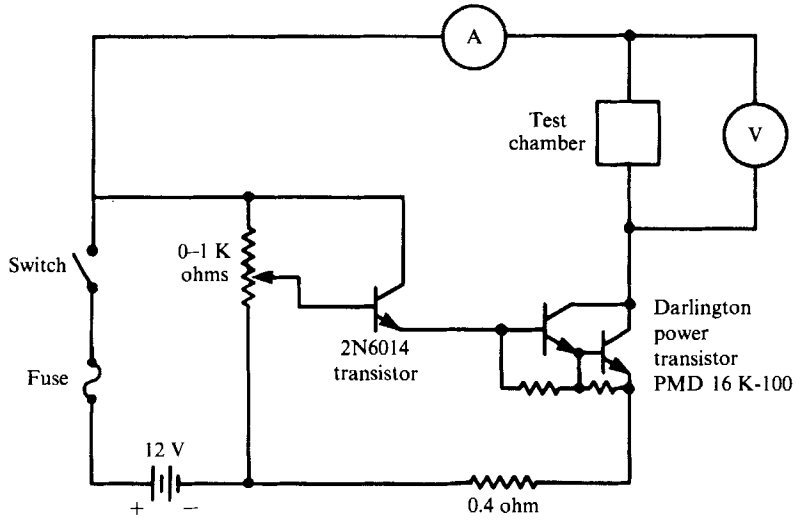

FIGURE 2. Schematic diagram of the electrical circuit.

The copper plates are each 33 cm × 48.3 cm × 0.635 cm (13 in. × 19 in. × $\frac{1}{4}$ in.). To the back of each plate, a 1.27 cm ($\frac{1}{2}$ in.) thick Plexiglas of the same size is attached. At the centre of each plate, a copper rod is attached onto the back of the copper plate through the Plexiglas. The copper rods are used as lead wires. Glyptal, an insulating enamel, is painted over all metal surfaces except the front. Spacers of different heights are used to control the separation between the two copper plates. Four Plexiglas pieces of thickness 1.27 cm ($\frac{1}{2}$ in.) are epoxied into rectangular-shaped spacers for placement along the border of the copper plates. The inner dimensions of all spacers are 30.5 cm × 45.7 cm (12 in. × 18 in.), which is also the active surface area of the copper plates. For the present study, the maximum spacing between the electrodes (fluid layer thickness) is 35.6 cm (14 in.).

A schematic of the electrical circuit is shown in figure 2. The power supply includes a 12 V automotive battery which along with a Darlington power transistor, a 2N6014 transistor, and a 0–1 kΩ multi-turn potentiometer provides the constant current source. An HP 414A analog display autovoltmeter and a Weston model 901 multi-range d.c. ammeter are used to measure the potential across, and the current through, the test fluid, respectively.

Before each run, both plates are polished with 600 grade emery paper, cleansed first with tap water, then with distilled water, and finally degreased with methanol-technical. The lower plate (cathode) and the appropriate spacer are placed in the housing which is inside the tank. Pre-mixed test solution is put into the tank to a level of about 4 cm above the top of the spacer. The upper plate (anode) is then lowered onto the housing with special care to avoid trapping any air inside the test section. The plate–spacer assembly is locked in place and more solution is added. After allowing time for the electrode and the solution to reach thermal equilibrium the temperature of the solution is measured using a mercury-in-glass thermometer.

For each test, the variation of current with potential difference is obtained to determine the limiting current. The test begins at low current and progresses to higher values. At each current setting, convection in the test cell is allowed to reach steady state; then the value of current and potential are recorded. Soon after the

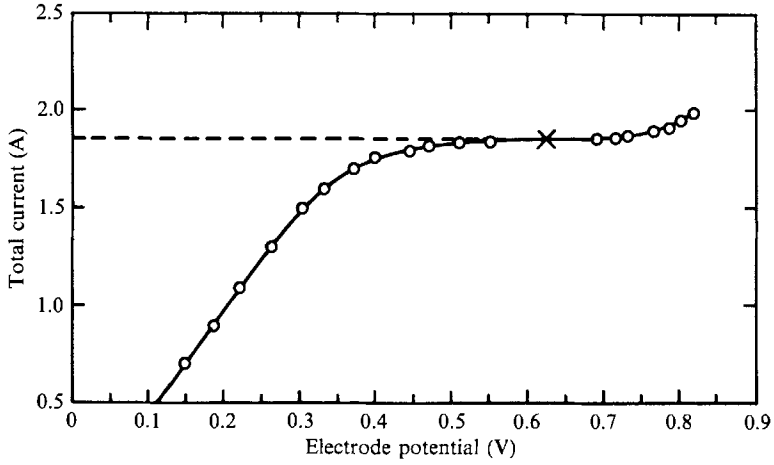

FIGURE 3. Current–voltage characteristic curve for run no. 21. $C_{CuSO_4} = 0.0252$ M, $L = 8.89$ cm, $I_{lim} = 1.331$ mA/cm^2.

establishment of the limiting current plateau, the experiment is terminated. A typical limiting current plot is given in figure 3.

After each test, the top electrode is removed and the temperature measured again to ensure constant temperature during the run. Three samples of the test solution are then extracted from the test section for analysis to determine the bulk concentration. Finally, the solution is emptied from the tank, and the test section is removed and cleaned. The bulk concentrations of the test solution are determined by standard chemical titration techniques.

4. Results

Tables 3(*a*) and 3(*b*) are tabulations of the present experimental runs for a horizontal layer at high Rayleigh numbers. In table 3(*a*), runs with three different nominal concentrations of cupric sulphate, 0.02 M, 0.025 M and 0.05 M are reported. For each cupric sulphate concentration, 16 runs were performed over a range of plate spacings from 1.27 cm to 35.6 cm. In table 3(*b*), eight runs at a nominal concentration of 0.0135 M for cupric sulphate are reported. The range of plate spacings used was from 1.27 cm to 10.2 cm. The results are plotted as *Sh vs. Ra* in figure 4.

The $\frac{1}{3}$-power law (equation (1)) and the definitions of *Sh* and *Ra* imply that the mass transfer coefficient is independent of the layer thickness L. This would hold for a given electrochemical solution at a fixed temperature. The rate of mass transfer is constant under fully-turbulent conditions where the $\frac{1}{3}$-power law holds. For the present study, this requires a constant limiting current density for a given concentration and temperature (Chiang & Goldstein 1990). From table 3(*a*), it can be seen that the limiting current density is essentially independent of the layer thickness within experimental uncertainties for $10^9 < Ra < 10^{13}$. The agreement with a $\frac{1}{3}$-power law might be examined more quantitatively by considering the variation of K calculated individually for each test run according to equation (1). These are also listed in tables 3(*a*) and 3(*b*) (cf. equations (15) and (16)).

At the lowest concentration (0.133 M), the data shows a small, but definite,

(*a*)

Run	C_{CuSO_4} (M)	$C_{H_2SO_4}$ (M)	T (°C)	I_{lim} (mA/cm^2)	L (cm)	Sc	Sh	$Ra \times 10^{-10}$	K
10	0.0198	1.477	18.9	0.969	5.08	2765	143.0	0.992	0.0665
11	0.0197	1.476	18.9	0.969	6.35	2765	179.6	1.927	0.0670
12	0.0198	1.476	19.0	0.980	7.62	2750	216.2	3.346	0.0671
13	0.0198	1.476	18.9	0.954	8.89	2760	246.2	5.315	0.0655
14	0.0197	1.478	19.1	0.947	10.16	2745	279.8	7.889	0.0652
15	0.0196	1.481	19.1	0.954	11.43	2740	318.5	11.17	0.0661
16	0.0197	1.480	19.6	0.969	12.70	2680	353.2	15.38	0.0659
17	0.0198	1.485	19.9	0.969	13.97	2645	383.8	20.54	0.0650
18	0.0198	1.485	19.1	0.965	15.24	2745	425.6	26.75	0.0660
19	0.0198	1.485	19.2	0.962	16.51	2730	458.0	33.99	0.0656
1A	0.0200	1.485	19.7	0.980	17.18	2670	475.0	38.62	0.0652
1B	0.0198	1.486	19.2	0.965	20.32	2730	565.9	63.37	0.0659
1C	0.0200	1.485	19.7	0.972	22.86	2670	627.4	90.99	0.0647
1D	0.0200	1.487	19.4	0.954	25.40	2700	688.7	124.9	0.0639
1E	0.0200	1.487	19.6	0.951	27.94	2685	752.3	166.2	0.0635
1F	0.0200	1.490	19.4	0.947	30.48	2710	821.9	215.9	0.0636
20	0.0253	1.445	19.7	1.349	7.62	2640	227.8	4.270	0.0652
21	0.0252	1.445	19.7	1.331	8.89	2650	263.6	6.754	0.0647
22	0.0252	1.445	19.7	1.342	10.16	2640	303.3	10.08	0.0652
23	0.0251	1.447	19.8	1.331	11.43	2635	339.4	14.29	0.0649
24	0.0252	1.448	19.6	1.331	12.70	2665	377.9	19.70	0.0649
25	0.0252	1.451	19.4	1.313	13.97	2690	412.2	26.24	0.0644
26	0.0251	1.449	19.7	1.342	15.24	2650	457.7	33.89	0.0657
27	0.0252	1.444	19.6	1.313	16.51	2660	484.3	43.28	0.0640
28	0.0252	1.455	19.4	1.313	17.78	2695	525.0	54.08	0.0644
29	0.0252	1.455	19.4	1.299	20.32	2685	592.6	80.71	0.0636
2A	0.0252	1.454	19.4	1.313	22.86	2685	673.9	114.9	0.0643
2B	0.0253	1.459	19.7	1.342	25.40	2660	758.4	158.1	0.0651
2C	0.0252	1.451	19.6	1.313	27.94	2665	820.7	209.7	0.0641
2D	0.0253	1.459	19.8	1.320	30.48	2645	892.9	273.1	0.0639
2E	0.0252	1.459	19.7	1.313	33.02	2660	968.6	346.0	0.0640
2F	0.0253	1.458	19.7	1.310	35.56	2660	1036.0	433.9	0.0635
30	0.0500	1.508	18.2	3.37	5.08	2965	204.2	2.519	0.0697
31	0.0500	1.508	18.2	3.30	6.35	2965	249.9	4.920	0.0682
32	0.0499	1.508	18.4	3.28	7.62	2935	297.1	8.478	0.0676
33	0.0500	1.507	18.6	3.28	8.89	2915	344.4	13.48	0.0672
34	0.0499	1.508	21.6	3.70	10.16	2520	411.1	19.85	0.0705
35	0.0499	1.508	21.3	3.52	11.43	2565	444.0	28.30	0.0676
36	0.0497	1.510	18.6	3.21	12.70	2910	484.3	39.06	0.0662
37	0.0497	1.510	18.5	3.19	13.97	2925	531.3	52.02	0.0661
38	0.0497	1.510	18.7	3.30	15.24	2895	595.7	67.47	0.0679
39	0.0497	1.510	18.3	3.12	16.51	2950	616.5	85.92	0.0648
3A	0.0498	1.509	19.9	3.51	17.78	2735	715.0	106.9	0.0699
3B	0.0498	1.510	20.8	3.40	20.32	2620	774.1	158.9	0.0663
3C	0.0496	1.510	19.1	3.29	22.86	2840	884.3	226.9	0.0673
3D	0.0497	1.509	19.9	3.44	25.40	2735	1002.0	310.9	0.0687
3E	0.0497	1.510	19.3	3.30	27.94	2810	1075.0	414.7	0.0669
3F	0.0497	1.509	20.0	3.43	30.48	2720	1197.0	537.0	0.0684

(*b*)

								$Ra \times 10^{-8}$	
1	0.0136	1.498	19.4	0.649	1.27	2695	34.44	1.061	0.0728
2	0.0133	1.498	19.4	0.615	2.54	2700	66.78	8.299	0.0711
3	0.0133	1.492	19.1	0.576	3.81	2735	94.43	28.05	0.0670
4	0.0133	1.492	18.6	0.578	5.08	2805	128.1	66.62	0.0681
5	0.0132	1.493	18.6	0.553	6.35	2810	154.5	129.1	0.0659
6	0.0132	1.491	18.6	0.548	7.62	2805	183.4	223.2	0.0651
7	0.0132	1.487	18.7	0.549	8.89	2780	213.5	354.2	0.0650
8	0.0133	1.494	19.3	0.563	10.16	2715	245.2	531.4	0.0652

TABLE 3. Present experimental runs for a horizontal layer at high Rayleigh numbers

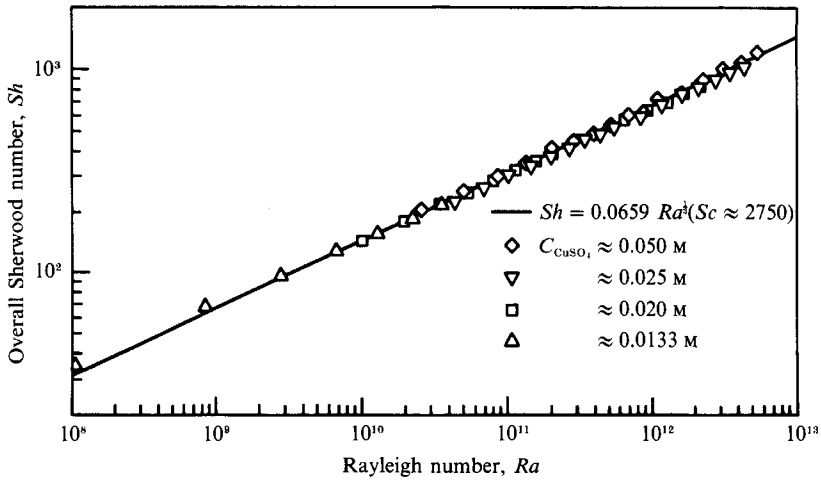

FIGURE 4. *Sh vs. Ra* for horizontal enclosures at high Rayleigh number.

increase in the limiting current density as the spacing L decreases. This can also be observed in figure 4 where all experimental points are plotted together with the best-fit $\frac{1}{3}$-power law correlation line (see equation (16) below). The two data points for $Ra < 10^9$ in figure 4 show a progressive deviation from the $\frac{1}{3}$-power law correlation. For moderate- to high-Prandtl-number fluids, at Rayleigh number between the first occurrence of chaotic flow and 10^9 the ability of thermals to penetrate to the opposite wall while retaining most of their identity may be the cause of the observed enhancement in the Nusselt or Sherwood number.

A least-square analysis of the data, excluding those from the two tests at $Ra < 10^9$, indicates a correlation

$$Sh = 0.0722\,Ra^{0.330} \quad (Sc \approx 2750), \tag{15}$$

with a standard deviation of 2.5% over 54 data points. The exponent is very close to $\frac{1}{3}$. A best-fit using the $\frac{1}{3}$-power law for the same data is

$$Sh = 0.0659\,Ra^{\frac{1}{3}} \quad (Sc \approx 2750). \tag{16}$$

This has a standard deviation of 2.6% for the same data.

The value of 0.0659 is 20% higher than the value of 0.0556 obtained for $Pr \approx 6.5$ (Goldstein & Tokuda 1980), suggesting a Prandtl (Schmidt) number dependence.

The proper form of the Prandtl (Schmidt) number dependence cannot be determined from just two values of K (0.0556 at Pr of 6.5 and 0.0659 at Sh (or Pr) of 2750). However, if a power law dependence on Pr is assumed, the exponent would be 0.0284.

5. Summary

The present paper presents a review of the literature on high-Rayleigh-number natural convection in a horizontal layer heated from below. The need for reliable data at high Rayleigh number and high Prandtl number leads to an experimental study using an electrochemical mass transfer technique. The high-Schmidt-number behaviour of the Sherwood–Rayleigh number correlation is examined. The results of the present study indicate a $\frac{1}{3}$-power correlation, $Sh = 0.0659\,Ra^{\frac{1}{3}}$ for $Sc \approx 2750$, and $3 \times 10^9 < Ra < 5 \times 10^{12}$.

The constant of proportionality obtained for the present study is about 20% higher than that obtained for water, $Nu = 0.0556 Ra^{\frac{1}{3}}$ for $Pr \approx 6.5$, suggesting a Prandtl (Schmidt) number dependence.

Support for this study was provided by the National Science Foundation.

REFERENCES

AHLERS, G. 1974 Low-temperature studies of the Rayleigh–Bénard instability and turbulence. *Phys. Rev. Lett.* **33**, 1185–1188.

ARPACI, V. S. 1986 Microscales of turbulence and heat transfer correlations. *Intl J. Heat Mass Transfer* **29**, 1071–1078.

BUSSE, F. H. 1969 On Howard's upper bound for heat transport by turbulent convection. *J. Fluid Mech.* **33**, 457–477.

CANUTO, V. M. & GOLDMAN, I. 1985 Analytical model for large-scale turbulence. *Phys. Rev. Lett.* **54**, 430–433.

CHAN, S.-K. 1971 Infinite Prandtl number turbulent convection. *Stud. Appl. Maths* **50**, 13–49.

CHANG, Y. P. 1957 A theoretical analysis of heat transfer in natural convection and in boiling. *Trans. ASME* **79**, 1501–1513.

CHIANG, H. D. & GOLDSTEIN, R. J. 1990 Application of the electrochemical mass transfer technique to the study of buoyancy-driven flows. (Submitted for publication.)

CHU, T. Y. & GOLDSTEIN, R. J. 1973 Turbulent natural convection in a horizontal water layer heated from below. *J. Fluid Mech.* **60**, 141–159.

DEARDORFF, J. W. 1965 A numerical study of pseudo three-dimensional parallel-plate convection. *J. Atmos. Sci.* **22**, 419–435.

DEARDORFF, J. W. & WILLIS, G. E. 1965 The effect of two-dimensionality on the suppression of thermal turbulence. *J. Fluid Mech.* **23**, 337–353.

DROPKIN, D. & SOMERSCALES, E. 1965 Heat transfer by natural convection in liquids confined by two parallel plates which are inclined at various angles with respect to the horizontal. *Trans. ASME* C: *J. Heat Transfer* **87**, 77–84.

FITZJARRALD, D. E. 1976 An experimental study of turbulent convection in air. *J. Fluid Mech.* **73**, 693–719.

FROMM, J. E. 1965 Numerical solutions of the non-linear equations for a heated fluid layer. *Phys. Fluids* **8**, 1757–1769.

GARON, A. M. & GOLDSTEIN, R. J. 1973 Velocity and heat transfer measurements in thermal convection. *Phys. Fluids* **16**, 1818–1825.

GLOBE, S. & DROPKIN, D. 1959 Natural convection heat transfer in liquids confined by two horizontal plates and heated from below. *Trans. ASME* **81**, 24–28.

GOLDSTEIN, R. J., CHIANG, H. D. & SAYER, E. 1987 Natural convection mass transfer in an inclined enclosure at high Rayleigh number. *2nd Intl Symp. on Transport Phenomena in Turbulent Flows, Tokyo, October 25–29, 1987.*

GOLDSTEIN, R. J. & CHU, T. Y. 1969 Thermal convection in a horizontal layer of air. *Prog. Heat Mass Transfer* **2**, 55–75.

GOLDSTEIN, R. J. & TOKUDA, S. 1980 Heat transfer by thermal convection at high Rayleigh numbers. *Intl J. Heat Mass Transfer* **23**, 738–740.

GOUGH, D. O., SPIEGEL, E. A. & TOOMRE, J. 1975 Modal equation for cellular convection. *J. Fluid Mech.* **68**, 695–719.

HERRING, J. R. 1964 Investigation of problems in thermal convection: rigid boundaries. *J. Atmos. Sci.* **21**, 277–290.

HESLOT, F., CASTAING, B. & LIBCHABER, A. 1987 Transitions to turbulence in helium gas. *Phys. Rev.* A **36**, 5870–5873.

HOLLANDS, K. G. T., RAITHBY, G. D. & KONICEK, L. 1975 Correlation equations for free convection heat transfer in horizontal layer of air and water. *Intl J. Heat Mass Transfer* **18**, 879–884.

HOWARD, L. N. 1963 Heat transport by turbulent convection. *J. Fluid Mech.* **17**, 405–432.

HOWARD, L. N. 1966 Convection at high Rayleigh number. *Proc. 11th Intl Congr. on Appl. Mech.*, pp. 1109–1115.

HOWARD, L. N. & KRISHNAMURTI, R. 1986 Large-scale flow in turbulent convection: a mathematical model. *J. Fluid Mech.* **170**, 385–410.

JAKOB, M. 1946 Free heat convection through enclosed plane gas layers. *Trans. ASME* **68**, 189–193.

KOSCHMIEDER, E. L. & PALLAS, S. G. 1974 Heat transfer through a shallow, horizontal convecting fluid layer. *Intl J. Heat Mass Transfer* **17**, 991–1002.

KRAICHNAN, R. H. 1962 Turbulent thermal convection at arbitrary Prandtl number. *Phys. Fluids* **5**, 1374–1389.

KRISHNAMURTI, R. 1973 Some further studies on the transition to turbulent convection. *J. Fluid Mech.* **60**, 285–303.

LEVICH, V. G. 1962 *Physicochemical Hydrodynamics.* Prentice-Hall.

LIPPS, F. B. 1976 Numerical simulation of three-dimensional Bénard convection in air. *J. Fluid Mech.* **75**, 113–148.

LONG, R. R. 1976 Relation between Nusselt number and Rayleigh number in turbulent thermal convection. *J. Fluid Mech.* **73**, 445–451.

MALKUS, W. V. R. 1954*a* Discrete transition in turbulent convection. *Proc. R. Soc. Lond.* A **225**, 185–195.

MALKUS, W. V. R. 1954*b* The heat transport and spectrum of thermal turbulence. *Proc. R. Soc. Lond.* A **225**, 196–212.

MIZUSHINA, T. 1971 The electrochemical method in transport phenomena. *Adv. Heat Transfer* **7**, 87–161.

MULL, W. & REIHER, H. 1930 Der Warmeschutz van Luftschichten. *Beihefte zum Gesundheits-Ingenieur* **1**, 28. Munich & Berlin.

NEWMAN, J. S. 1973 *Electrochemical Systems.* Prentice-Hall.

ROBERTS, P. H. 1966 On non-linear Bénard convection. In *Non-Equilibrium Thermodynamics, Variational Techniques, and Stability* (ed. R. Donnelly, R. Hermann & I. Prigogine), pp. 125–162. University of Chicago Press.

ROSSBY, H. T. 1969 A study of Bénard convection with and without rotation. *J. Fluid Mech.* **36**, 309–335.

SCHMIDT, E. & SILVESTON, P. L. 1959 Natural convection in horizontal liquid layer. *Chem. Engng Prog. Symp. Ser.* **55**, 163–169.

SELMAN, J. R. & TOBIAS, C. W. 1978 Mass transfer measurements by the limiting current technique. *Adv. Chem. Engng* **10**, 211–318.

SOMERSCALES, E. F. C. & GAZDA, I. W. 1968 Thermal convection in high Prandtl number liquids at high Rayleigh numbers. *Rensselaer Polytechnic Inst. ME Rep.* HT-5.

SPARROW, E. M., HUSAR, R. B. & GOLDSTEIN, R. J. 1970 Observations and other characteristics of thermals. *J. Fluid Mech.* **41**, 793–800.

SPIEGEL, E. A. 1962 On the Malkus theory of turbulence. In *Mécanique de la Turbulence, edition du CNRS Paris*, pp. 181–201.

SPIEGEL, E. A. 1967 The theory of turbulent convection. *28th IAU Symp.*, pp. 348–366. Academic.

STRAUSS, J. M. 1976 On the upper bounding approach to thermal convection of moderate Rayleigh number, II. Rigid boundaries. *Dyn. Atmos. Oceans* **1**, 77–90.

TANAKA, H. & MIYATA, H. 1980 Turbulent natural convection in a horizontal water layer heated from below. *Intl J. Heat Mass Transfer* **23**, 1273–1281.

THRELFALL, D. C. 1975 Free convection in low-temperature gaseous helium. *J. Fluid Mech.* **67**, 17–28.

TOWNSEND, A. A. 1959 Temperature fluctuations over a heated horizontal surface. *J. Fluid Mech.* **5**, 209–241.

TOWNSEND, A. A. 1962 Remarks on the Malkus theory of turbulent flow. In *Mécanique de la Turbulence, edition du CNRS Paris*, pp. 167–180.

WILLIS, G. E. & DEARDORFF, J. W. 1967 Confirmation and renumbering of the discrete heat flux transitions of Malkus. *Phys. Fluids* **10**, 1861–1866.

WRAGG, A. A. 1977 Application of the limiting diffusion current technique in chemical engineering. *Chem. Engnr (Lond.)* **316**, 39–44.

Review articles and papers

ADRIAN, R. J., FERREIRA, R. T. D. S. & BOBERG, T. 1986 Turbulent thermal convection in wide horizontal fluid layers. *Expt Fluids* **4**, 121–141.

BUSSE, F. H. 1978*a* The optimum theory of turbulence. *Adv. Appl. Mech.* **18**, 77–121.

BUSSE, F. H. 1978*b* Non-linear properties of thermal convection. *Rep. Prog. Phys.* **41**, 1929–1967.

BUSSE, F. H. 1981 Transition to turbulence in Rayleigh–Bénard convection. In *Hydrodynamic Instabilities and Transition to Turbulence*. Springer.

CATTON, I. 1978 Natural convection in enclosures. *Proc. 6th Intl Heat Transfer Conf. Toronto* **6**, 13–31.

CHANDRASEKHAR, S. 1961 *Hydrodynamic and Hydromagnetic Stability*. Clarendon Press.

DENTON, R. A. & WOOD, I. R. 1979 Turbulent convection between two horizontal plates. *Intl J. Heat Mass Transfer* **22**, 1339–1346.

GERSHUNI, G. Z. & ZHUKOVITSKII, E. M. 1976 *Convective Stability of Incompressible Fluids* (trans. from Russian by D. Louvish). Jerusalem: Keter.

JOSEPH, D. D. 1976 *Stability of Fluid Motions*, vols 1 and 2. Springer.

KOSCHMEIDER, E. L. 1974 Bénard convection. *Adv. Chem. Phys.* **26**, 177–212.

NORMAND, C., POMEAU, Y. & VELARDE, M. G. 1977 Convective instability: a physicist's approach. *Rev. Mod. Phys.* **49**, 581–624.

PALM, E. 1975 Nonlinear thermal convection. *Ann. Rev. Fluid Mech.* **7**, 39–61.

PRIESTLEY, C. H. B. 1959 *Turbulent Transfer in the Lower Atmosphere*. University of Chicago Press.

RAITHBY G. D. & HOLLANDS, K. G. T. 1985 Natural convection. In *Handbook of Heat Transfer Fundamentals*, 2nd edn, ch. 6.

SEGEL, L. A. 1966 Non-linear hydrodynamic stability theory and its applications to thermal convection and curved flows. In *Non-Equilibrium Thermodynamics, Variational Techniques and Stability* (ed. R. Donnelly, R. Herman & I. Prigogine), pp. 165–197. University of Chicago Press.

SPIEGEL, E. A. 1971 Convection in stars: I. Basic Boussinesq convection. *Ann. Rev. Astro. Astrophys.* **9**, 323–352.

SPIEGEL, E. A. 1972 Convection in stars: II. Special effects. *Ann. Rev. Astro. Astrophys.* **10**, 261–304.

SUTTON, O. G. 1953 *Micrometerology*. McGraw-Hill.

TURNER, J. S. 1973 *Buoyancy Effects in Fluids*. Cambridge University Press.